# Tanshinone IIA protects against chronic obstructive pulmonary disease via exosome-shuttled miR-486-5p

DONGDONG TIAN[1], YINGCHUN MIAO[2], WENDONG HAO[1], NING YANG[1], PING WANG[1], QINGYI GE[3] and CAILIAN ZHANG[1]

[1]Department of Respiratory, The Affiliated Hospital of Yan'an University; [2]Department of Emergency, Yan'an Hospital of Traditional Chinese Medicine, Yan'an, Shaanxi 716000; [3]School of Clinical Medicine, Harbin Medical University, Harbin, Heilongjiang 150081, P.R. China

Received August 13, 2021; Accepted January 11, 2022

DOI: 10.3892/ijmm.2022.5153

**Abstract.** Chronic obstructive pulmonary disease (COPD) is one of the major causes of death worldwide today, and its related morbidity has been predicted to show an increase in subsequent years. Recent studies have shown that Danshen, a Chinese herbal medicine, is a potential drug in the treatment of inflammation-related lung diseases. COPD was induced in this study using cigarette smoke (CS) exposure plus intranasal inhalation of lipopolysaccharide to ascertain whether the main pharmacological component from Danshen, tanshinone IIA (TIIA), and its water soluble form, sodium tanshinone IIA sulfonate (STS), protect against the development of COPD. The weight, lung function, hematoxylin and eosin staining, and Masson Trichrome determinations revealed that TIIA inhalation attenuated lung dysfunction in COPD mice induced by cigarette smoke and lipopolysaccharide exposure. In addition, exosomes derived from TIIA-treated COPD mice exerted similar protective effects against COPD, suggesting that TIIA may protect against COPD through exosome-shuttled signals. miR-486-5p was found to be a key molecule in mediating the protective effects of exosomes derived from TIIA-treated COPD mice using miRNA sequencing and cellular screening. Treatment of COPD mice with an agomiR of miR-486-5p protected lung function in COPD mice, and treatment of COPD mice with an antagomir of miR-486-5p abolished the protective effects of TIIA. Moreover, luciferase activity reporter assay, RT-qPCR, and western blot analyses showed that miR-486-5p exerted protective effects against COPD via targeting phosphoinositide-3-kinase regulatory subunit 1 (*PIK3R1*). These results suggest that STS protects against COPD through upregulation of miR-486-5p, and that TIIA or miR-486-5p is a potential drug for the treatment of COPD.

*Correspondence to:* Dr Cailian Zhang, Department of Respiratory, The Affiliated Hospital of Yan'an University, 250 North Street, Yan'an, Shaanxi 716000, P.R. China
E-mail: zhangcailiandoc@126.com; zcl@yau.edu.cn

*Key words:* chronic obstructive pulmonary disease, tanshinone IIA, miR-486-5p, PIK3R1, lung injury treatment

## Introduction

Chronic obstructive pulmonary disease (COPD) is one of the major causes of death worldwide today, and its related morbidity has been predicted to show an increase in the following years (1). It is a preventable and treatable disease which shows progressive and not fully reversible airflow limitation, and it is associated with chronic inflammatory responses and oxidative stress to poisonous particles or gases in the airway and lung (2,3). Tobacco smoking, including second-hand smoke exposure, is the main risk factor for COPD, contributing to 90% of COPD-related deaths (4). The other risk factor for COPD include environmental conditions, such as dust and fumes. Downregulating airway smooth-muscle tone using bronchodilators and/or reducing pulmonary inflammation using inhaled corticosteroids or phosphodiesterase type 4 inhibitors (e.g., roflumilast) is the major strategy for the treatment of COPD at present (5). These drugs are expensive and display adverse side effects, which limit their clinical use (6,7). Previous studies indicate that microRNAs (miRNAs) are involved in the pathogenetic and therapeutic progression of COPD (8), which provide a promising new therapeutic approach targeting at the inflammatory response and/or oxidative stress to prevent and treat patients with COPD.

Recent studies have shown that Danshen, a Chinese herbal medicine and the dried root of *Savia miltiorrhiza*, is a potential drug for the treatment of inflammation-related lung diseases (9,10). Danshen has been widely used in many countries including China, Japan and the US to treat various diseases, including cardiovascular diseases, chronic liver diseases, bronchitis and stroke (11). Tanshinone IIA (TIIA), the main pharmacological component from Danshen, has been shown to exert profound anti-inflammatory and anti-oxidative effects in lung and cardiac diseases in animal studies (12-14). In addition, a recent study showed that TIIA inhalation exerted protective effects against cigarette smoke (CS) and lipopolysaccharide (LPS) exposure-induced COPD in mice, attenuating lung function decline, airspace enlargement, mucus production, bronchial collagen deposition, inflammatory responses

and oxidative stress through downregulation of cystic fibrosis transmembrane conductance regulator (10). These advances suggest that TIIA is a potential drug for the treatment of COPD with high efficiency and low side effects. Sodium tanshinone IIA sulfonate (STS) is a water-soluble derivative of TIIA. Similar to TIIA, STS has been reported to have anti-oxidative and anti-inflammatory activities (15), which makes it a promising therapeutic agent for COPD. However, the underlying mechanism of STS involved in the protective effects against COPD is largely unknown.

Different from Western medicine, Chinese medicine consistently shows multiple target and systemic effects through which it exerts protective effects against diseases, suggesting that the systemic effects of TIIA may contribute to its protective effects against COPD. Exosomes, small (30-100 nm) endogenous membrane vesicles secreted by most cell types, play important roles in mediating cell-to-cell communication and crosstalk between organs via shuttling proteins, mRNAs, and non-coding RNAs (such as miRNAs) (16-18). Exosomes have emerged as novel elements that mediate the therapeutic effects of various strategies (19-21). The role of exosomes in the mediation of the effects of Chinese medicine has also been examined (22). A study by Ruan *et al* demonstrated that Suxiao Jiuxin pill treatment significantly increased exosome secretion (23). Maremanda *et al* demonstrated that exosomes derived from mesenchymal stem cells showed a protective effect to cigarette smoke-induced mitochondrial dysfunction in mice (24). These advances suggest that exosomes may play a role in the mediation of the protective effects of TIIA against COPD. Here, we examined the role of exosomes in the protective effects of TIIA in COPD mice, and found that TIIA protects against COPD via exosome-shuttled miR-486-5p.

## Materials and methods

*Induction of COPD in C57 mice and treatment*. A total of 132 wild-type C57 male mice (age 6-8 weeks and weight 20±3 g) were purchased from the Beijing Vital River Laboratory Animal Technology Co., Ltd. and used in the induction of COPD. All animals were housed in a specified pathogen-free and temperature controlled (24±2˚C temperature and 55% humidity) condition with 12 h-12 h light/dark cycles and free access to food and water. Animal experiments were approved by the Animal Care and Use Committee of Yan'an University (Yan'an, Shaanxi, China) following ICUAC guidelines. COPD was induced as reported previously (10). Briefly, the COPD model was established using CS exposure plus intranasal inhalation of lipopolysaccharide (LPS). LPS (7.5 $\mu$g/mouse in 50 $\mu$l saline; L8643, Sigma-Aldrich) or saline (vehicle control) was administered to the mice by intranasal inhalation on the 1st and 14th day. CS (9 cigarettes/h, 2 h/session, twice/day and 6 days/week in a whole-body exposure chamber) was administered to the mice from day 0 to 60 except for the days giving LPS. The cigarettes used were Plum brand filtered cigarettes (Guangdong Tobacco Industry) and each cigarette yields 11 mg tar, 1.0 mg nicotine and 13 mg carbon monoxide.

For TIIA treatment, sodium tanshinone IIA sulfonate (STS) (Jiangsu Carefree Pharmaceutical), a water-soluble substance derived from TIIA, was used. Mice were administered saline or STS (5 mg/kg, 30 min per session, twice per day) by airway inhalation with a PARI Nebuliser (PARI GmbH) in a whole-body exposure chamber for 30 min daily before being exposed to CS. Finally, all mice were subjected to lung function analysis, and sacrificed at day 61.

For exosome treatment, exosomes purified from equal volumes (1 ml) of plasma was intravenous injected into mice at an interval of every 7 days from the 1st day of COPD induction. For miR-486-5p intervention, agomir or antagomir of miR-486-5p (1 nmol) was intravenously injected into mice at an interval of every 7 days from the 1st day of COPD induction. For sacrifice, the mice were euthanized using $CO_2$ exposure with 3 liters/min (~45% volume/min) flow rate, and $CO_2$ exposure lasted for more than 1 min after breathing was determined to be arrested.

*Measurement of lung function*. Lung function was evaluated using the Forced Pulmonary Maneuver System (Buxco Research Systems) as described previously (10). Mice were anesthetized with pentobarbital (50 mg/kg body weight). The breathing frequency was set at 150 breaths/min. Three semiautomatic maneuvers were used. These included: Boyle's law functional residual capacity maneuver to detect functional residual capacity, quasi-static pressure volume maneuver to detect total lung capacity and chord compliance, and fast flow volume maneuver to detect forced expiration volume in 50 msec and forced vital capacity.

*Hematocrit measurement*. Capillary tubes (0.5-mm outside diameter, VWR Scientific) was used to collect blood via right ventricle puncture with $K_2$EDTA as an anticoagulant. The collected blood was centrifuged at 300 x g for 5 min, and read using a hematocrit chart (VWR Scientific).

*Histopathology*. The left lung specimens of the mice were isolated and fixed in 10% neutral buffered formalin for 24 h, embedded in paraffin wax, and cut into 4-$\mu$m thick slices. The slices were stained with hematoxylin and eosin (H&E; Nanjing Jiancheng Bioengineering) to evaluate morphological changes and Masson Trichrome (Nanjing Jiancheng Bioengineering) to detect collagen deposition of small airways according to manufacturer's instructions.

*Plasma exosome isolation and characterization*. Blood samples were taken from mice with COPD. Plasma exosomes were isolated using the ExoQuick Plasma prep and the Exosome Precipitation kit according to the manufacturer's instructions (System Biosciences). The isolated exosomes were resuspended in PBS for further experiments. Transmission electron microscopy was conducted as previously described (22), and Nanoparticle tracking analysis (NTA) was carried out using a NanoSight NS300 (Marvel).

*miRNA sequencing*. miRNA sequencing was performed by Guangzhou RiboBio Co., Ltd. Briefly, adaptors were added to the 30 and 50 end of total RNAs extracted from plasma. Then, products of reverse transcription polymerase chain reaction (RT-PCR) derived from 18- to 30- nt RNAs were purified. The Illumina Hiseq 2500 platform (Illumina, Inc.) was used for the sequencing.

*Cell culture*. Human bronchial epithelial 16HBE cells were purchased from the Cell Bank of the Chinese Academy of Sciences (Shanghai, China) and cultured with DMEM (Biological Industries Israel Beit Haemek, Ltd.) supplemented with 10% FBS (Thermo Fisher Scientific, Inc.), 100 $\mu$g/ml penicillin and 100 $\mu$g/ml streptomycin (Beyotime Institute of Biotechnology) in a humidified incubator at 37˚C with 95% (v/v) air and 5% (v/v) $CO_2$.

*Cigarette smoke extract (CSE) preparation and exposure*. CSE was freshly prepared from Plum brand filtered cigarettes within 30 min prior to treatments as reported previously (10). The acquired CSE suspension in yellowish color with an optical density (OD) at 405 nm (0.506±0.008) was adjusted to pH 7.4, passed through a 0.22-$\mu$m filter to remove bacteria and particles and considered as concentration 100% in cell treatments. The cells were exposed to CSE (2%) for 12 h.

*RT-qPCR*. Total RNA was extracted from plasma by an RNA isolation kit (AccuRef Scientific) according to the manufacturer's instructions. Equal amounts of RNA were added to a reverse transcriptase reaction mix (Takara), with oligo-dT as a primer. The resulting templates were subjected to PCR using SYBR Green Master Mix kit (AccuRef Scientific) in ABI 7500 Real-Time PCR system (Applied Biosystems; Thermo Fisher Scientific, Inc.) with the following conditions: 95˚C for 10 min and 40 cycles of 95˚C for 5 sec, 58˚C for 20 sec, and 72˚C for 10 sec. Using actin (mRNA specific) or U6 (miRNA) as the internal control, the relative expression of genes was calculated using the $2^{-\Delta\Delta Cq}$ method (25). Specific primers used are shown in Table SI.

*Cell transfection*. miR-22-3p mimic (5'-AAGCUGCCAGUU GAAGAACUGU-3'), miR-486-5p mimic (5'-UCCUGUACU GAGCUGCCCCGAG-3'), miR-16-5p mimic (5'-UAGCAG CACGUAAAUAUUGGCG-3'), miR-10b-5p mimic (5'-UAC CCUGUAGAACCGAAUUUGUG-3'), miR-27b-3p mimic (5'-UUCACAGUGGCUAAGUUCUGC-3'), miRNA negative control (miR-NC; cat. #B04001), agomir-NC (cat. #B04008), agomiR-486-5p (cat. #B06001), antagomiR-NC (cat. #B04007), and antagomiR-486-5p (cat. #B05001) were synthesized by GenePharma Company (Shanghai, China). miRNA mimic (100 nmol/l) or miR-NC (100 nmol/l) was transfected using Lipofectamine™ 3000 (Invitrogen; Thermo Fisher Scientific, Inc.) according to the manufacturer's protocol. After 48 h of transfection, cells were harvested and used for further experiments.

*Dual-luciferase reporter assay*. Wild-type (Wt) and mutant (Mt) *PIK3R1* 3' UTR sequence was obtained by PCR amplification using template and primers, and then cloned into *Spe*I and *Hin*dIII sites of the pMir-Report Luciferase vector (Applied Biosystems; Thermo Fisher Scientific, Inc.). The resulting construct was transfected (5 ng) into macrophages with 20 nM control mimics or 20 nM mimics for miR-486-5p using Lipofectamine 2000 (Invitrogen; Thermo Fisher Scientific, Inc.) according to the manufacturer's instructions. After 24 h of transfection, luciferase activity in the cells was determined using a Luciferase Assay System (Promega Corp.).

*Apoptosis analysis*. After transfected with miRNA mimic/NC, PIK3R1, and/or treatment with CSE, the apoptotic cells were measured using the Annexin V-FITC/PI apoptosis Detection kit (Beyotime Institute of Biotechnology) according to the manufacturer's protocol. Briefly, adherent and suspension cultured 16HBE cells were harvested and centrifuged at 1,000 x g at 4˚C for 5 min followed by cold PBS rinse for three times. Then, cells were re-suspended in 200 $\mu$l of suspension buffer and incubated with 5 $\mu$l of Annexin V-FITC and 5 $\mu$l of PI at room temperature for 20 min in the dark. Following this, suspension buffer was added to 1 ml and analyzed using flow cytometry (Beckman Coulter).

*CCK-8 assay*. After transfected with miRNA mimic/NC or PIK3R1 for 48 h, the cells were seeded into 96-well plates at a density of $1.0x10^4$ per well and cultured for 24 h. Then, the cells were treated with CSE or/and STS for 48 h. After incubation, 10 $\mu$l of CCK-8 solution (Beyotime Institute of Biotechnology) was added to each well and incubated at 37˚C for 2 h. Then, the optical density (OD) value of each well was detected at 450 nm using a microplate reader (BioTek).

*Western blot analysis*. Protein expression was measured using western blot analysis. Briefly, cells and tissues were lysed on ice for 30 min using RIPA lysis buffer and centrifuged at 4˚C and 12,000 x g for 10 min, and proteins (the supernatants) were quantified using the BCA method (AccuRef Scientific). Then, 25 $\mu$g protein for each sample was diluted in loading buffer (EXINNO) and subjected to 12% SDS-PAGE followed by electronic transferring to PVDF membrane. Subsequently, the membranes were blocked with 5% skimmed milk solution at room temperature for 30 min and probed with anti-CD63 (dilution: 1:200; cat. no. SAB4301607; Sigma-Adrich; Merck KGaA), anti-CD81 (dilution: 1:1,000; cat. no.ab109201; Abcam), anti-phosphoinositide-3-kinase regulatory subunit 1 (PIK3R1, dilution: 1:1,000; cat. no. ab191606; Abcam) or anti-β-actin (dilution: 1:1,000; cat. no. ab8226; Abcam) overnight at 4˚C followed by incubation with the corresponding anti-mouse secondary antibody (dilution: 1:5,000; cat. no. ab6728; Abcam) or anti-rabbit secondary antibody (dilution: 1:5,000; cat. no. ab6721; Abcam) at room temperature for 1 h. The blots were visualized with ECL-Plus Reagent (AccuRef Scientific). Finally, the protein bands on membranes were quantified using ImageJ software (version 1.49, NIH) for further statistical analysis.

*Statistical analysis*. All values are presented as mean ± standard deviation. Data between two groups were compared using an unpaired t-test. Data among multiple groups were compared using one-way analysis of variance (ANOVA) followed by Turkey's post hoc with Bonferroni's correction to reduce the dominance of type-I error. Differences were considered significant at $P<0.05$.

## Results

*STS inhalation protects against COPD*. After 60 days of induction, COPD mice displayed typical clinical manifestations, including decreased body weight (Fig. 1A), increased lung weight (Fig. 1B), impaired lung function (Fig. 1C-H) and

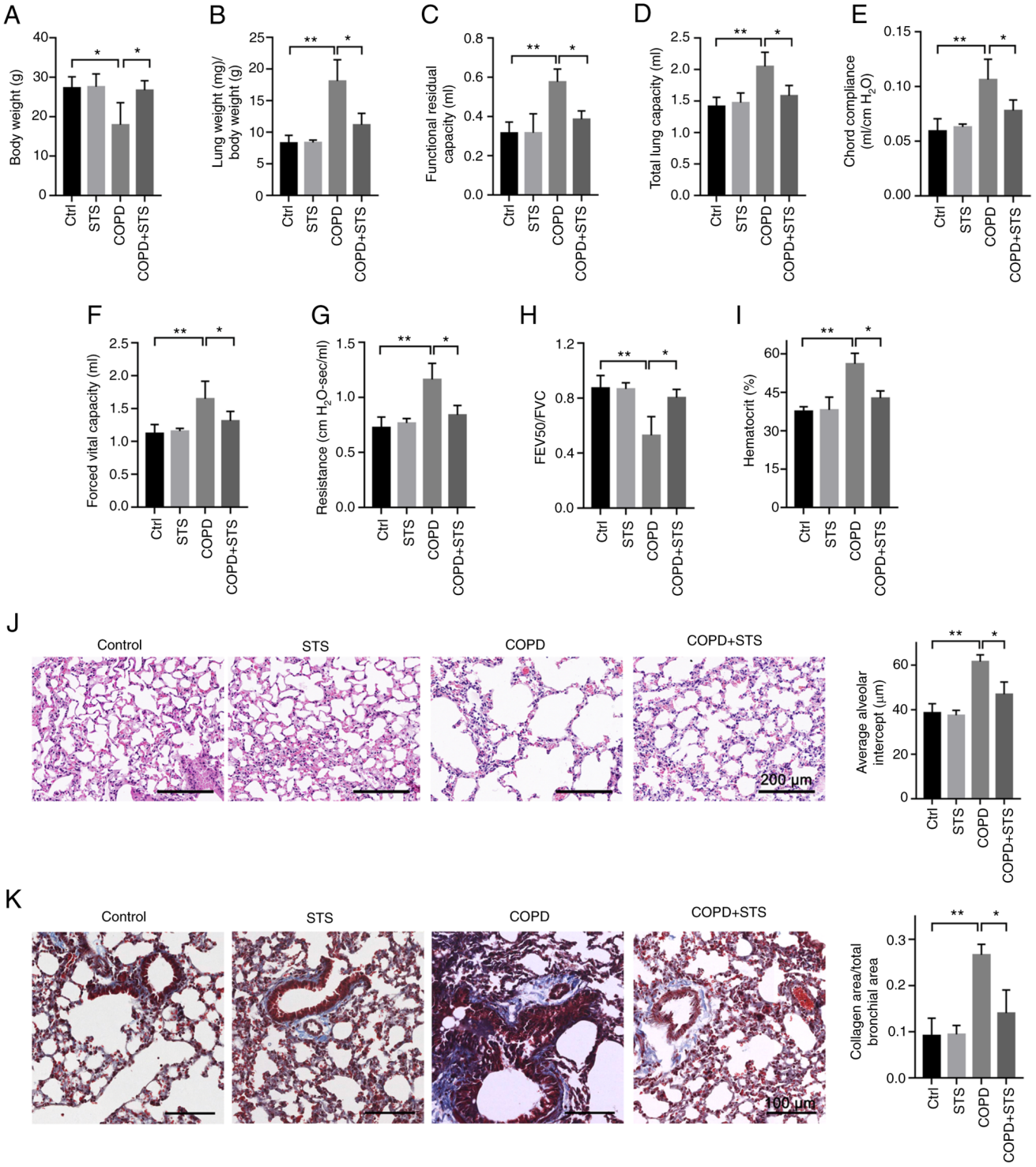


Figure 1. STS inhalation protects against COPD. (A) Body weight of the COPD mice. (B) Lung weight of the COPD mice. (C-H) STS inhalation improved lung function in the COPD mice as indicated by parameters of functional residual capacity (C), total lung capacity (D), chord compliance (E), forced vital capacity (F), lung resistance (G), and forced expiratory volume at 50 msec (H). (I) Hematocrit value in blood in the COPD mice. (J) STS inhalation decreased pulmonary structural damage as detected by H&E staining. (K) STS inhalation decreased collagen deposition in the small airway as detected by Masson staining. n=6. $^{*}$P<0.05 and $^{**}$P<0.01. COPD, chronic obstructive pulmonary disease; STS, sodium tanshinone IIA sulfonate.

increased hematocrit value in blood (Fig. 1I). An impairment of lung function was evidenced by increases in functional residual capacity (Fig. 1C), total lung capacity (Fig. 1D), chord compliance (Fig. 1E), forced vital capacity (Fig. 1F) and lung resistance (Fig. 1G), a decrease in forced expiratory volume at 50 msec (Fig. 1H), and an increased hematocrit value in blood (Fig. 1I). All of these manifestations were attenuated in mice with STS inhalation when compared to the vehicle-treated mice (Ctrl) (Fig, 1A-I). In addition, the protective effects of STS were further manifested by a decrease in pulmonary structural damage as detected by H&E staining (Fig. 1J), as well as a decrease in collagen deposition in the small airway as detected by Masson staining (Fig. 1K). The lung of COPD mice displayed damaged alveolar walls, pulmonary bullae

and increased collagen deposition which were attenuated in STS-treated mice (Fig. 1J and K). These results demonstrated that STS inhalation exerted protective effects against CS-LPS exposure-induced COPD.

*Exosomes derived from STS-treated COPD mice exert protective effects against COPD*. To test whether exosomes contribute to the protective effects of STS, exosomes were purified from the plasma of COPD mice treated with or without STS. Electron microscopy revealed typical rounded particles (50-100 nm in diameter) in isolated fractions (Fig. 2A). Nanoparticle tracking showed no differences in size distribution and plasma concentration between exosomes derived from untreated COPD and STS-treated COPD mice (Fig. 2B and C), and the results were further confirmed by western blot analysis (Fig. 2D). Then, purified exosomes were administrated to COPD mice to test whether these exosomes exert protective effects against COPD. Interestingly, exosomes purified from STS-treated COPD mice exerted protective effects against COPD. Exosome treatment increased body weight (Fig. 2E), improved lung function (Fig. 2F-L) and decreased hematocrit value in blood (Fig. 2M) in mice with COPD, while exosomes treatment showed little effects in the control (Ctrl) mice (Fig. 2F-M). In addition, the protective effects of exosomes were further manifested by a decrease in pulmonary structural damage as detected by H&E staining (Fig. 2N), as well as a decrease in collagen deposition in the small airway as detected by Masson staining (Fig. 2O). Particularly, exosomes purified from STS-treated COPD mice showed higher protective effects than that from the untreated COPD mice (Fig. 2E-O), suggesting that there were endogenous protective factors in the exosomes of COPD mice and STS treatment enhanced their protective effects.

*Exosome-shuttled miR-486-5p protects lung cells in vitro*. To explore the possibility of miRNA(s) contributing to exosome-mediated protective effects against COPD, a miRNA profiling assay comparing the differences between exosomes purified from untreated COPD and STS-treated COPD mice was conducted using Illumina HiSeq 2500 high-throughput sequencing. A total of 417 differentially expressed miRNAs (fold change >1.5; $P<0.05$; Fig. 3A) were detected, and the top 5 were further confirmed by RT-qPCR (Fig. 3B). Among these miRNAs, miR-22-3p, miR-486-5p, and miR-27b-3p were upregulated in the exosomes purified from the STS-treated COPD mice compared with those in the untreated COPD mice, while miR-16-5p was significantly downregulated in the exosome derived from the STS treated COPD mice compared with the COPD mice (Fig. 3B). We further tested these 5 miRNAs in 16HBE cells. The results demonstrated that overexpression of these five miRNAs had no obvious effect on the cell viability and apoptosis of the 16HBE cells (Fig. 3C-E). However, overexpression of miR-486-5p significantly increase the cell viability and decreased apoptosis of the 16HBE cells after exposure to CSE (Fig. 3F and G). To validate the interaction between exosome and lung epithelial cells, 16HBE cells were treated with exosomes purified from COPD mice (COPD-exo) or STS-treated COPD mice (COPD+STS-exo). We found significantly increased viability in the COPD+STS-exo group when compared with the viability in the exosomes derived from COPD mice (COPD-exo) group (Fig. S1). These results suggest that exosome-shuttled miR-486-5p may mediate the protective effects of STS against COPD.

*miR-486-5p protects against COPD*. Agomir of miR-486-5p was used by intravenous injection to upregulate the level of miR-486-5p in COPD mice to test whether miR-486-5p protects against COPD. As shown in Fig. 4A, miR-486-5p was upregulated in both the control (Ctrl) and COPD mice, suggesting that the injection of miR-486-5p agomir was successfully performed (Fig. 4B-I). Further analyses showed that agomiR-486-5p treatment increased body weight (Fig. 4B), improved lung function (Fig. 4C-I) and decreased the hematocrit value in blood (Fig. 4J) in COPD mice compared with that in untreated COPD mice, while agomiR-486-5p treatment showed little effects in the control mice (Fig. 4B-J). In addition, the protective effects of agomiR-486-5p were further confirmed by a decrease in pulmonary structural damage as detected by H&E staining (Fig. 4K), as well as a decrease in collagen deposition in the small airway as detected by Masson staining (Fig. 4L). These results demonstrated that miR-486-5p protects against COPD in mice.

*STS protects against COPD through upregulation of miR-486-5p*. Antagomir of miR-486-5p was used by intravenous injection to downregulate the level of miR-486-5p in STS-treated COPD mice to test whether miR-486-5p contributes to the protective effects of STS against COPD. As shown in Fig. 5A, miR-486-5p was downregulated in STS-treated COPD mice by antagomiR-486-5p treatment, and downregulation of miR-486-5p in STS-treated COPD mice attenuated the protective effects of STS against COPD (Fig. 5B-I). AntagomiR-486-5p treatment decreased body weight in the STS-treated COPD mice, while it showed little effects on body weight in COPD mice without STS treatment (Fig. 4B). AntagomiR-486-5p treatment decreased lung function (Fig. 5C-I) and increased the hematocrit value in blood (Fig. 5J) in the STS-treated COPD mice. In addition, the effects of antagomiR-486-5p were further confirmed by an increase in pulmonary structural damage as detected by H&E staining (Fig. 5K), as well as an increase in collagen deposition in the small airway as detected by Masson staining (Fig. 5L). These results demonstrated that STS protects against COPD through upregulation of miR-486-5p.

*miR-486-5p exerts protective effects against COPD via targeting PIK3R1*. Target genes of miR-486-5p were predicted by miRmap (http://mirnamap.mbc.nctu.edu.tw/), microT (http://diana.imis.athena-innovation.gr/DianaTools/index.php?r=microT_CDS/index), TargetScan (http://www.targetscan.org/mamm_31/) and PicTar (https://pictar.mdc-berlin.de/). There were 10 candidates (Fig. 6A). The miR-486-5p mimic decreased *PIK3R1* mRNA level more significantly in 16HBE cells (Fig. 6B). PIK3R1 is a subunit of phosphatidylinositol 3-kinase (PI3K) and regulates PI3K activity. The binding sites for miR-486-5p in the 3'-untranslated regions (3'UTRs) of *PIK3R1* were further examined using a luciferase reporter assay. Either wild-type (WT) 3'UTRs or mutant (MUT) 3'UTRs in putative miR-486-5p binding sites were cloned into a reporter plasmid and assessed their responsiveness to

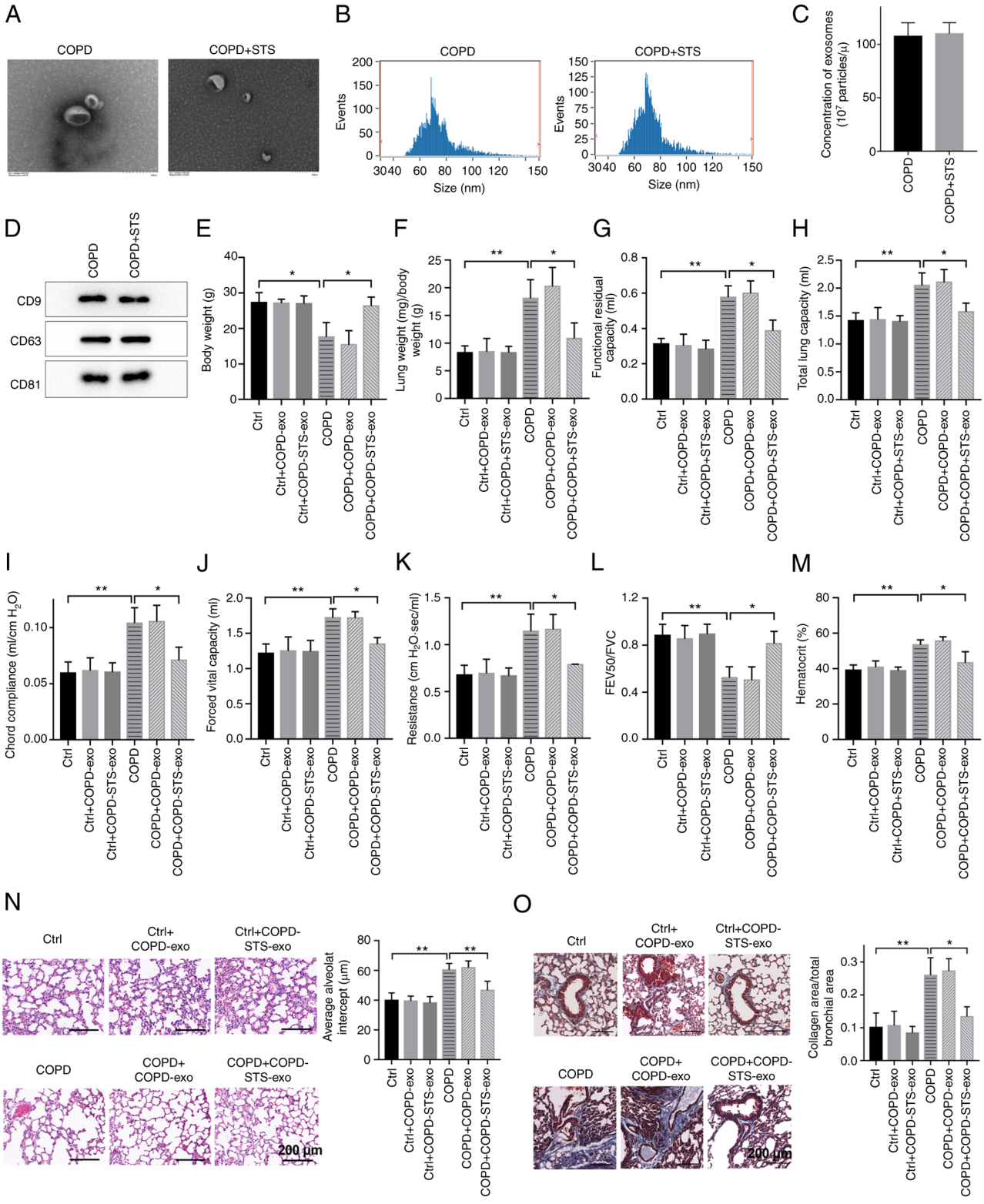


Figure 2. Exosomes derived from STS-treated COPD mice exert protective effects against COPD. (A) Electron microscopy revealed typical rounded particles (50-100 nm in diameter) in isolated exosomes. (B and C) Nanoparticle tracking showed no differences in size distribution (B) and plasma concentration (C) between exosomes derived from untreated COPD and STS-treated COPD mice. (D) Western blot analysis of exosome markers. (E) Body weight of the COPD mice. (F) Lung weight of the COPD mice. (G-L) Exosomes purified from the STS-treated COPD mice improved lung function in COPD mice as indicated by parameters of functional residual capacity (G), total lung capacity (H), chord compliance (I), forced vital capacity (J), lung resistance (K), and forced expiratory volume at 50 msec (L). (M) Hematocrit value in blood in the COPD mice. (N) Exosomes purified from STS-treated COPD mice decreased pulmonary structural damage as detected by H&E staining. (O) Exosomes purified from STS-treated COPD mice decreased collagen deposition in the small airway as detected by Masson staining. n=6. $^{*}$P<0.05 and $^{**}$P<0.01. COPD, chronic obstructive pulmonary disease; STS, sodium tanshinone IIA sulfonate.

miR-486-5p in 293T cells. The results showed that miR-486-5p reduced luciferase activity for PIK3R1 wild-type 3'UTR constructs but had no effect when the miR-486-5p binding sites were mutated (Fig. 6C and D). RIP assay showed that PIK3R1

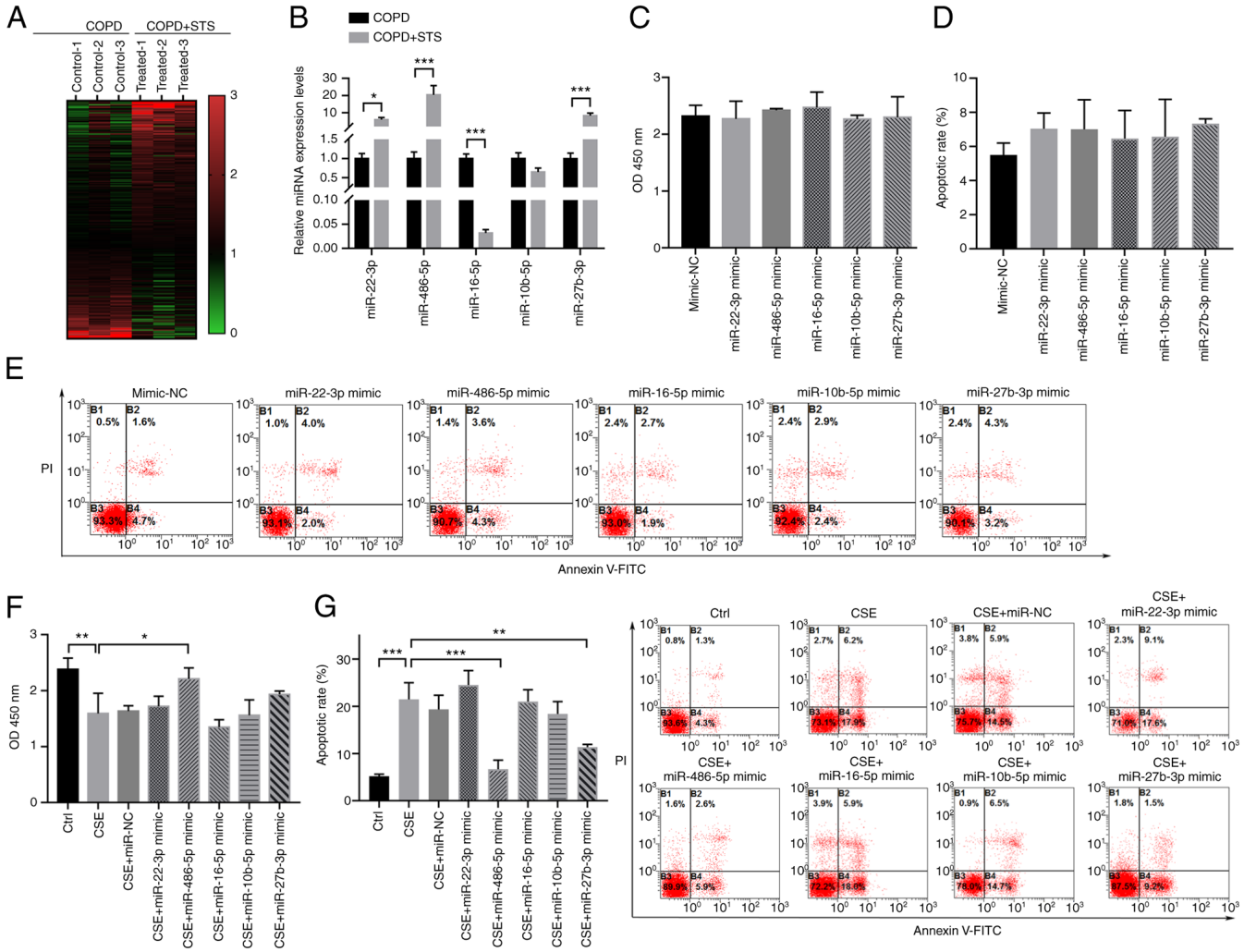


Figure 3. Exosome-shuttled miR-486-5p protects lung cells *in vitro*. (A) miRNA profiling assay comparing the differences between exosomes purified from untreated COPD and STS-treated COPD mice. (B) The differentially expressed miRNAs were confirmed by RT-qPCR. (C-E) Cell viability (C) and apoptosis (D and E) following overexpression of the miRNAs in normal 16HBE cells. (F) miR-486-5p increased cell viability in the CSE-exposed 16HBE cells. (G) miR-486-5p decreased cell apoptosis in the CSE-exposed 16HBE cells. n=4. $^{*}$P<0.05, $^{**}$P<0.01 and $^{***}$P <0.001. COPD, chronic obstructive pulmonary disease; STS, sodium tanshinone IIA sulfonate; CSE, cigarette smoke extract; OD optical density.

could directly interact with miR-486-5p (Fig. 6E). Following this, expression of PIK3R1 was determined in 16HBE cells after transfection with miR-486-5p (Fig. 6F). The results showed that overexpression of miR-486-5p could significantly inhibit *PIK3R1* mRNA expression (Fig. 6G). Protein levels in 16HBE cells detected by western blot analysis showed the same trends consistent with the results of the mRNA levels (Fig. 6H), indicating PIK3R1 as a potential target of miR-486-5p. We also tested the expression levels of PIK3R1 in mice. PIK3R1 expression was upregulated in the COPD mice, and STS treatment decreased PIK3R1 expression in the COPD mice (Fig. 6I). Exosomes purified from untreated and STS-treated COPD mice also decreased PIK3R1 expression in the COPD mice (Fig. 6J). AgomiR-486-5p decreased PIK3R1 expressions and antagomir-486-5p increased PIK3R1 expressions in the COPD mice (Fig. 6K and L). These results demonstrated that miR-486-5p exerts protective effects against COPD via targeting PIK3R1.

*Overexpression of PIK3R1 attenuates the protective effect of STS-induced miR-486-5p in CSE-exposed 16HBE cells*. To further explore the role of PIK3R1 in COPD, PIK3R1 was overexpressed in 16HBE cells and exposed to CSE followed by cell viability and apoptosis analyses. The result demonstrated that PIK3R1 was significantly upregulated in the 16HBE cells and CSE exposure could further enhance the expression of PIK3R1 in 16HBE cells (Fig. 7A). Cell viability analysis showed that overexpression of PIK3R1 could significantly inhibit the viability of 16HBE cells and CSE exposure markedly enhanced this reduction in the cell viability of 16HBE cells (Fig. 7B). Western blot analysis demonstrated that overexpression of PIK3R1 significantly enhanced the expression of cleaved-PARP, cleaved-caspase-3, and cleaved-caspase-9, but had no obvious effect on the expression of pro-PARP, pro-caspase-3, and pro-caspase-9 in 16HBE cells exposed to CSE (Fig. 7C). In addition, further flow cytometric analysis showed that PIK3R1 expression significantly increased the apoptosis of 16HBE cells and CSE exposure could significantly aggregate the apoptosis of the PIK3R1-overexpressed 16HBE cells (Fig. 7D). These findings demonstrated that overexpression of PIK3R1 enhanced the CSE-induced injury in 16HBE cells.

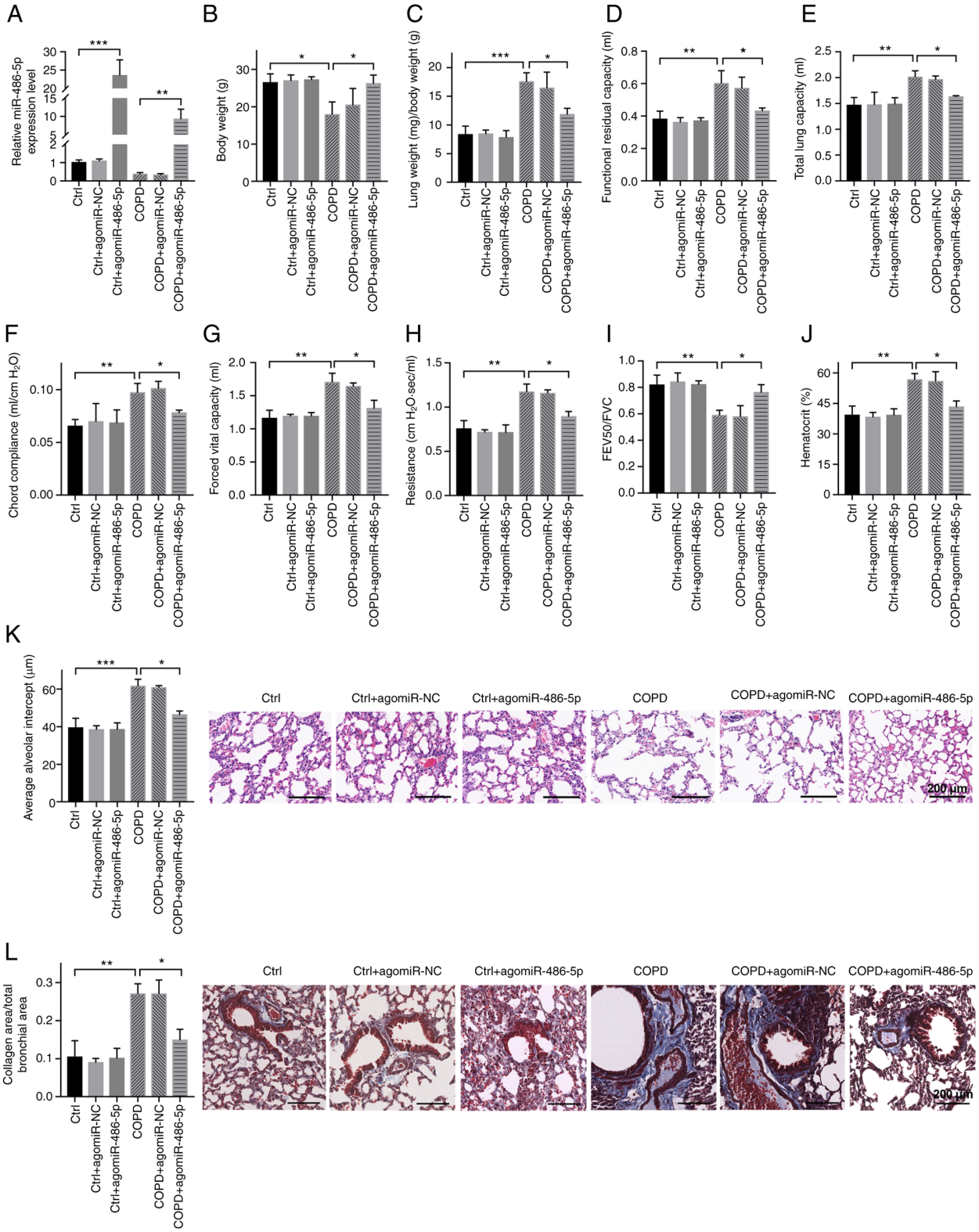


Figure 4. miR-486-5p protects against COPD. (A) miR-486-5p was upregulated by an agomir of miR-486-5p in the COPD mice. (B) Body weight of the COPD mice. (C) Lung weight of the COPD mice. (D-I) AgomiR-486-5p improved lung function in the COPD mice as indicated by parameters of functional residual capacity (D), total lung capacity (E), chord compliance (F), forced vital capacity (G), lung resistance (H), and forced expiratory volume at 50 msec (I). (J) Hematocrit value in the blood in COPD mice. (K) AgomiR-486-5p decreased pulmonary structural damage as detected by H&E staining in the COPD mice. (L) AgomiR-486-5p decreased collagen deposition in the small airway as detected by Masson staining in the COPD mice. n=6. $^{*}$P<0.05; $^{**}$P<0.01 and $^{***}$P<0.001. COPD, chronic obstructive pulmonary disease.

To reveal whether STS could alleviate COPD injury via the miR-486-5p/PIK3R1 axis, miR-486-5p and PIK3R1 were co-transfected into CSE-exposed 16HBE cells and treated with STS. The result presented that STS treatment could obviously abort PIK3R1 upregulation induced by CSE and overexpression of PIK3R1 could reverse the effect of STS, but overexpression

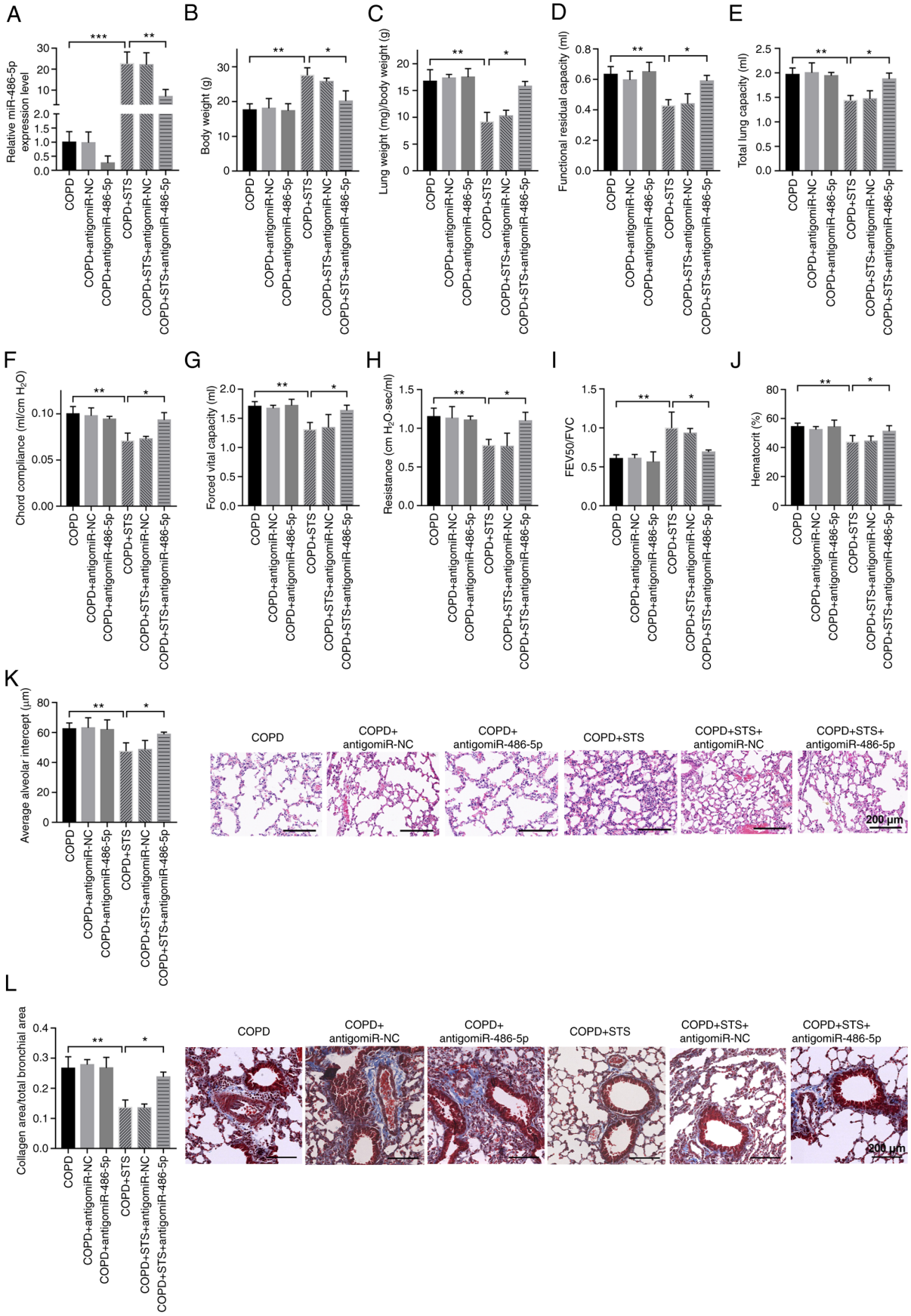


Figure 5. STS protects against COPD through upregulation of miR-486-5p. (A) miR-486-5p was downregulated in STS-treated COPD mice by antagomiR-486-5p treatment. (B-J) Downregulation of miR-486-5p in STS-treated COPD mice attenuated the protective effects of STS against COPD. Body weight (B), lung weight (C), functional residual capacity (D), total lung capacity (E), chord compliance (F), forced vital capacity (G), lung resistance (H), forced expiratory volume at 50 msec (I), and hematocrit value in blood (J) are shown. (K) AntagomiR-486-5p increased pulmonary structural damage as detected by H&E staining in STS-treated COPD mice. (L) AntagomiR-486-5p increased collagen deposition in the small airway as detected by Masson staining in STS-treated COPD mice. n=6. $^{*}$P<0.05; $^{**}$P<0.01 $^{***}$P<0.001. COPD, chronic obstructive pulmonary disease; STS, sodium tanshinone IIA sulfonate.

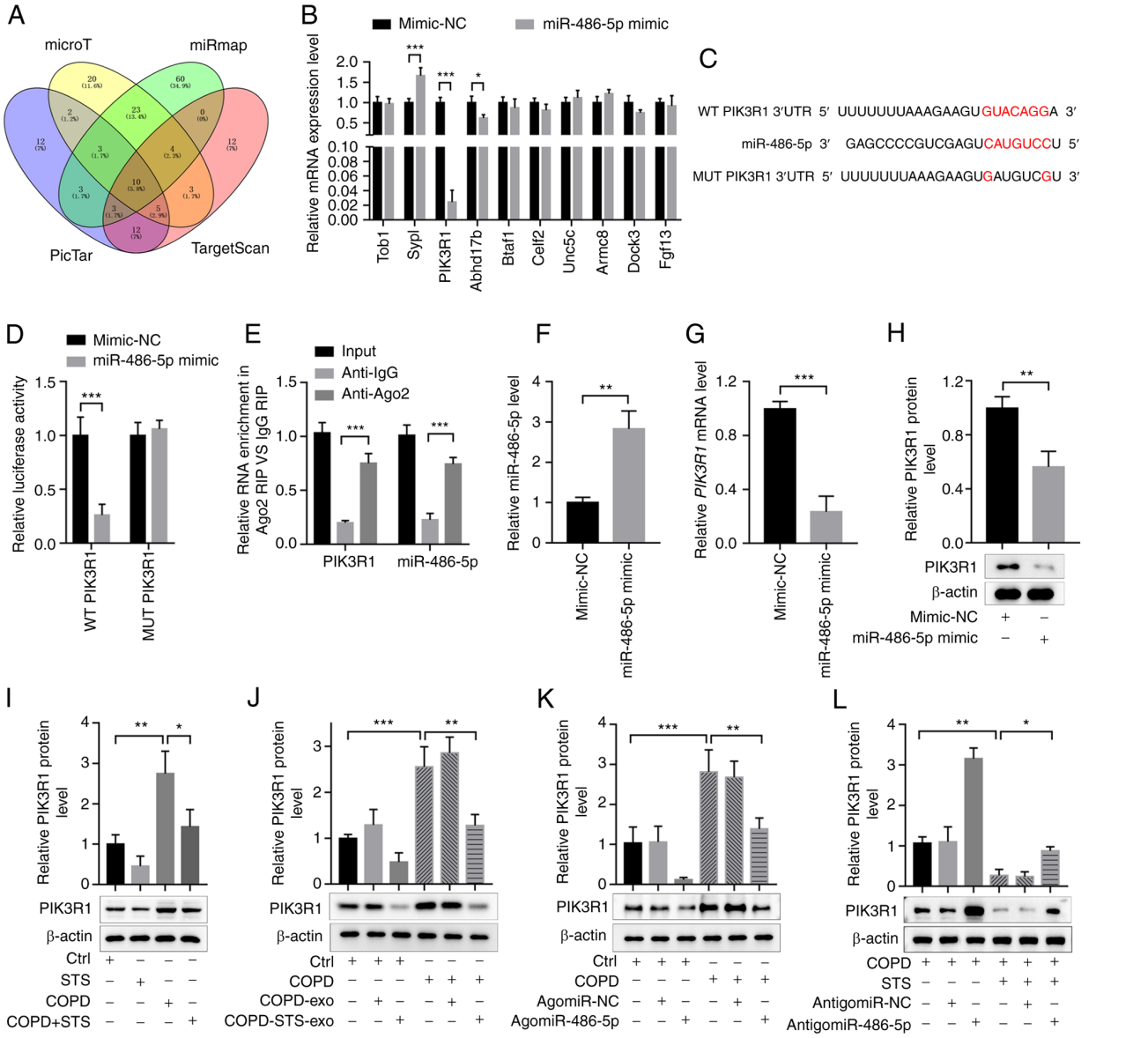


Figure 6. miR-486-5p exerts protective effects against COPD via targeting PIK3R1. (A) Target genes of miR-486-5p were predicted by miRmap, microT, TargetScan and PicTar. (B) The miR-486-5p mimic decreased *PIK3R1* mRNA levels more significantly in 16HBE cells. (C and D) The binding sites for miR-486-5p in the 3'-untranslated region (3'UTR) of *PIK3R1* were examined using a luciferase reporter assay. (E) RIP assay revealed the direct interaction between miR-486-5p and 3'UTR of *PIK3R1* mRNA. (F) Confirmation of miR-486-5p overexpression in 16HBE cells. (G and H) miR-486-5p regulated *PIK3R1* mRNA (G) and protein (H) levels in 16HBE cells. (I) PIK3R1 protein levels in COPD mice treated with STS. (J) PIK3R1 protein levels in COPD mice treated with exosomes purified from COPD mice. (K) PIK3R1 protein levels in COPD mice treated with agomiR-486-5p. (L) PIK3R1 protein levels in COPD mice treated with antogomiR-486-5p. n=4. $^{*}$P<0.05; $^{**}$P<0.01 and $^{***}$P<0.001. COPD, chronic obstructive pulmonary disease; PIK3R1, phosphoinositide-3-kinase regulatory subunit 1; STS, sodium tanshinone IIA sulfonate.

of miR-486-5p remarkably decreased PIK3R1 expression in the PIK3R1-overexpressing 16HBE cells after exposure to CSE and treatment with STS (Fig. 7E). Cell viability analysis showed that STS treatment could significantly promote the viability of CSE-exposed 16HBE cells and PIK3R1 could attenuate the effect of STS on the viability of 16HBE cells, while overexpression of miR-486-5p could abort PIK3R1 effect on the viability of CSE and STS co-treated 16HBE cells (Fig. 7F). Flow cytometry also demonstrated that STS could decrease the apoptosis of 16HBE cells exposed to CSE and overexpression of PIK3R1 could attenuate the protective effect of STS; however, miR-486-5p reversed the effect of PIK3R1 and rescued the protective effect of STS (Fig. 7G). In addition, western blot analysis presented that STS treatment significantly decreased the upregulation of cleaved-PARP, cleaved-caspase-3, and cleaved-caspase-9 induced by CSE, but had no marked effect on the expression of pro-PARP, pro-caspase-3, and pro-caspase-9 in the 16HBE cells. However, PIK3R1 overexpression could obviously attenuate the protective effect of STS and miR-485-5p could attenuate the effect of PIK3R1 to rescue the protective effect of STS (Fig. 7H). All of these data demonstrated that STS alleviated the CSE-induced injury in 16HBE cells via regulating the miR-485-5p/PIK3R1 axis.

## Discussion

Danshen and its derivative products including its water soluble form, sodium tanshinone IIA sulfonate (STS), have been

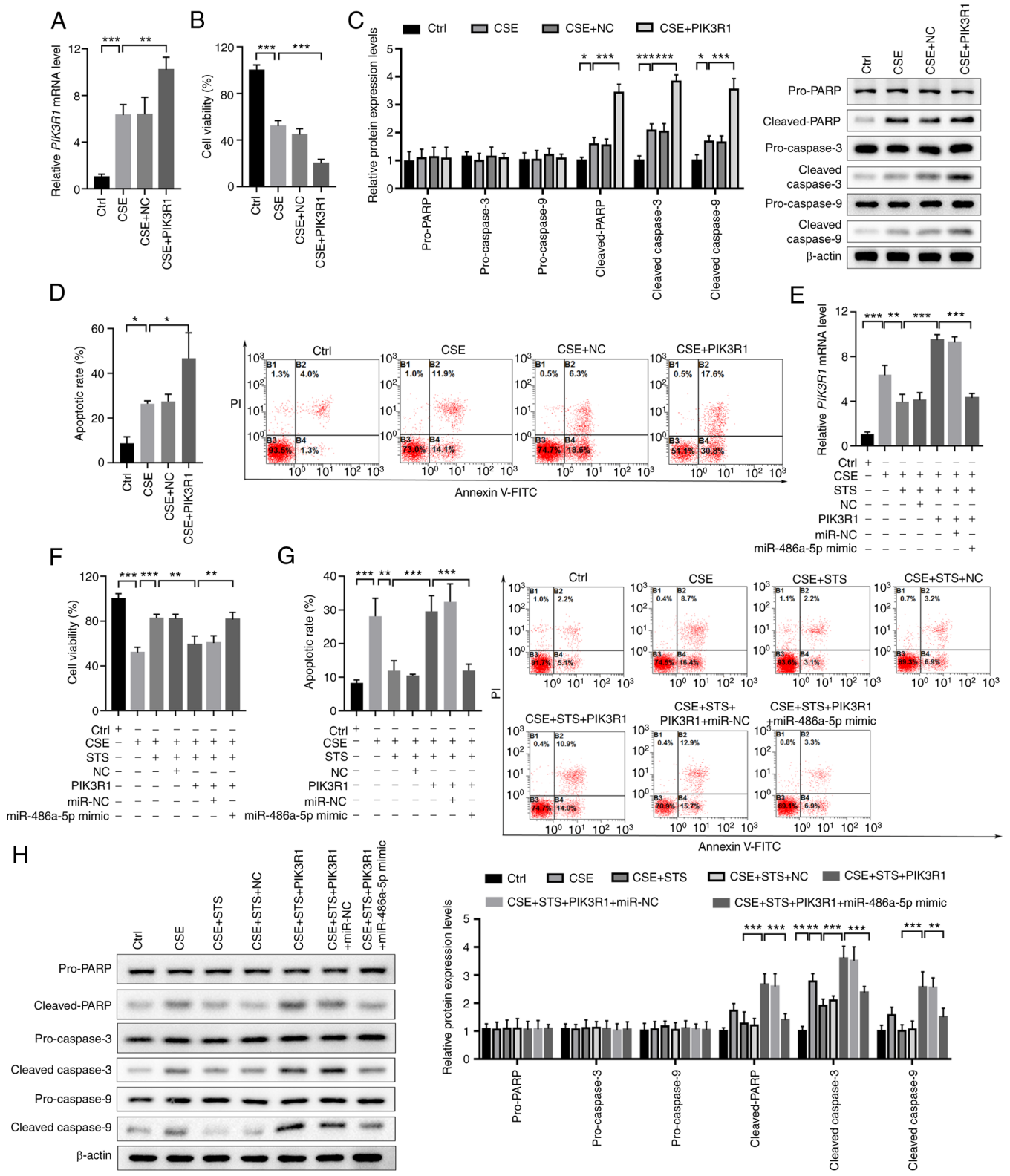


Figure 7. STS protects 16HBE cells against CSE-induced injury via the miR-486-5p/PIK3R1 axis. (A) Confirmation of *PIK3R1* overexpression in CSE-exposed 16HBE cells. (B) Cell viability of CSE-exposed 16HBE cells with or without *PIK3R1* overexpression. (C) Expression of apoptotic markers in CSE-exposed 16HBE cells with or without *PIK3R1* overexpression. (D) Apoptosis of CSE-exposed 16HBE cells with or without *PIK3R1* overexpression. (E) Expression of *PIK3R1* in 16HBE cells after exposure to CSE, treatment with STS, PIK3R1 overexpression, or miR-486-5p overexpression. (F and G) Cell viability (F) and apoptosis (G) of 16HBE cells after exposure to CSE, treatment with STS, *PIK3R1* overexpression, or miR-486-5p overexpression. (H) Expression of apoptotic markers in 16HBE cells after exposure to CSE, treatment with STS, *PIK3R1* overexpression, or miR-486-5p overexpression. $^{*}$P<0.05, $^{**}$P<0.01 and $^{***}$P<0.001. COPD, chronic obstructive pulmonary disease; PIK3R1, phosphoinositide-3-kinase regulatory subunit 1; STS, sodium tanshinone IIA sulfonate; CSE, cigarette smoke extract.

applied to treat cardiovascular and cerebrovascular diseases in the clinic. Recent research has shown that STS exerted protective effects against COPD in rodents (10). The present study demonstrated that STS inhalation attenuated lung

dysfunction in mice with COPD, and its protective effects were mediated by the elevation of circulating miR-486-5p via targeting PIK3R1. The results suggest that STS is a potential drug for the clinical treatment of COPD.

STS has been described as an antioxidant to reduce oxidative stress and inflammatory responses, which scavenges oxygen-free radicals, prevents lipid peroxidation, inhibits low density lipoprotein oxidation, increases Zn superoxide dismutase (SOD) activity as well as mRNA and protein expression, activates the Nrf2 pathway and inhibits NF-κB and MAPK signaling pathways (26-28). In the present study, we found that STS treatment significantly reduced lung injury responses to CS exposure. These findings are consistent with a previous study (10). A broad spectrum of anti-inflammatory drugs, including inhibitors of the pro-inflammatory enzymes PDE4, Janus kinases, NF-κB kinase, p38 mitogen-activated protein kinase, and PI3 kinase-γ and -δ, have been developed for COPD treatment, but their side effects limit their clinical application (29). Unlike significant advances in the development of long-acting bronchodilators, it has proven difficult to find safe and effective anti-inflammatory treatments for COPD. As a medicine used in traditional Chinese medicine, the side effects and safety of Danshen and Danshen products have been fully evaluated in clinical practice (11). Indeed, we found that the dose of STS used in the study to treat COPD did not cause a detectable toxic effect. Based on our findings, STS is a potential drug for preventing COPD, which could be conveniently delivered by aerosol inhalation.

It has been shown that STS protects COPD through downregulation of cystic fibrosis transmembrane conductance regulator in local lungs (10). Our study extended the findings that STS protects against COPD through upregulation of miR-486-5p which is derived from circulation, suggesting that various factors both from local and circulation are involved in the protective effects of STS against COPD. miRNAs are endogenous noncoding small RNAs (~22 nt) that modulate the activity of mRNA by hybridizing to complementary sequences in the 3'-untranslated region (UTR) of specific targets (30). Numerous studies have demonstrated that miRNAs participate in various cell biological processes, including cell growth, differentiation, and cell apoptosis and various interventions exert beneficial effects through regulation of miRNAs (31,32). Thus, it is possible for STS to exert beneficial effects through regulation of miRNAs. Indeed, there are reports which show the contribution of miRNAs in the beneficial effects of Chinese medicine (33-35). Here, our miRNA sequencing data revealed that miR-22-3p, miR-486-5p, and miR-27b-3p were upregulated, while miR-16-5p was downregulated in the exosomes derived from STS-treated COPD mice. Among the significantly altered miRNAs, miR-22-3p and miR-486-5p were reported to have anti-inflammatory effects (36-38), while miR-27b-3p and miR-16-5p are involved in the initiation of inflammation (39,40). In the present study, we found that STS exerted beneficial effects through upregulation of miR-486-5p. Our ongoing research will be to investigate other exosome-derived miRNAs found in this study, under which the potential mechanisms would provide further understanding of the beneficial effect of STS for preventing COPD.

miR-486-5p has been extensively studied in tumors, including lung cancer. Various studies have shown that miR-486-5p is downregulated in lung cancers (41-44). Upregulation of miR-486-5p reduces tumor proliferation and migration. PIK3R1 is a well-established target of miR-486-5p in various pathological conditions. PIK3R1 is a subunit of PI3K which plays an important role in the regulation of a vast array of fundamental cellular processes, including proliferation, adhesion, cell size, and protection from apoptosis (45,46). Although PI3K signaling exerts protective effects in various diseases, recent studies demonstrated that PI3K signaling is prominently activated in COPD and correlates with an increased susceptibility of patients to lung infections (47,48). PI3K isoforms have emerged as promising alternative drug targets for respiratory diseases, including COPD, and a wide array of pan-isoform and isoform-selective inhibitors have been tested in preclinical models and are currently being evaluated in clinical studies (47). Consistently with previous studies, our results showed that PI3K is overactivated in COPD as evidenced by the increased expression of PIK3R1. Although the role of PIK3R1 has not been explored in COPD, its role in lung cancer has been extensively studied. *PIK3R1* is the 11th most commonly mutated gene across cancer lineages in the TCGA database (49). Various studies have shown that miR-486-5p is downregulated and PIK3R1 is upregulated in lung cancers (41-44). Upregulation of miR-486-5p or PIK3R1 abrogation reduces tumor proliferation and migration. These advances reinforce the notion that the miR-486-5p/PIK3R1 axis plays an important role in the regulation of lung function.

Taken together, these results demonstrated that STS inhalation effectively attenuated CS-induced lung dysfunction in COPD, and STS-elevated miR-486-5p contributes to its protective effects against COPD via targeting PIK3R1. These findings extend the current knowledge that STS exerts protective effects through systemic alterations. Thus, STS is a potential drug for the treatment of COPD.

**Acknowledgements**

Not applicable.

**Funding**

This study was supported by the National Natural Science Foundation of China (no. 81860014).

**Availability of data and materials**

The datasets used and/or analyzed during the present study are available from the corresponding author upon reasonable request.

**Authors' contributions**

DT and CZ conceived and designed the study. DT, YM, WH, NY, PW and QG performed the experiments and statistical analyses. DT and CZ wrote the paper. YM, WH, NY, and PW reviewed and edited the manuscript. All authors read and approved the manuscript and agree to be accountable for all aspects of the research in ensuring that the accuracy or integrity of any part of the work, including the data, are appropriately investigated and resolved.

## Ethics approval and consent to participate

Animal experiments were approved by the Animal Care and Use Committee of Yan'an University (Yan'an, Shaanxi, China) following ICUAC guidelines.

## Patient consent for publication

Not applicable.

## Competing interests

All the authors declare that they have no competing interests.

## References


1. Lozano R, Naghavi M, Foreman K, Lim S, Shibuya K, Aboyans V, Abraham J, Adair T, Aggarwal R, Ahn SY, *et al*: Global and regional mortality from 235 causes of death for 20 age groups in 1990 and 2010: A systematic analysis for the global burden of disease study 2010. Lancet 380: 2095-2128, 2012.
2. Miravitlles M, Calle M and Soler-Cataluña JJ: Clinical phenotypes of COPD: Identification, definition and implications for guidelines. Arch Bronconeumol 48: 86-98, 2012 (In English, Spanish).
3. Vestbo J: COPD: Definition and phenotypes. Clin Chest Med 35: 1-6, 2014.
4. Salvi S: Tobacco smoking and environmental risk factors for chronic obstructive pulmonary disease. Clin Chest Med 35: 17-27, 2014.
5. Calverley PM: New treatments for COPD: Many miles still to go. Lancet Respir Med 2: 6-7, 2014.
6. Tamimi A, Serdarevic D and Hanania NA: The effects of cigarette smoke on airway inflammation in asthma and COPD: Therapeutic implications. Respir Med 106: 319-328, 2012.
7. Page CP and Spina D: Selective PDE inhibitors as novel treatments for respiratory diseases. Curr Opin Pharmacol 12: 275-286, 2012.
8. De Smet EG, Mestdagh P, Vandesompele J, Brusselle GG and Bracke KR: Non-coding RNAs in the pathogenesis of COPD. Thorax 70: 782-791, 2015.
9. Li J, Zheng Y, Li MX, Yang CW and Liu YF: Tanshinone IIA alleviates lipopolysaccharide-induced acute lung injury by downregulating TRPM7 and pro-inflammatory factors. J Cell Mol Med 22: 646-654, 2018.
10. Li D, Wang J, Sun D, Gong X, Jiang H, Shu J, Wang Z, Long Z, Chen Y, Zhang Z, *et al*: Tanshinone IIA sulfonate protects against cigarette smoke-induced COPD and down-regulation of CFTR in mice. Sci Rep 8: 376, 2018.
11. Zhou L, Zuo Z and Chow MS: Danshen: An overview of its chemistry, pharmacology, pharmacokinetics, and clinical use. J Clin Pharmacol 45: 1345-1359, 2005.
12. Long R, You Y, Li W, Jin N, Huang S, Li T, Liu K and Wang Z: Sodium tanshinone IIA sulfonate ameliorates experimental coronary no-reflow phenomenon through down-regulation of FGL2. Life Sci 142: 8-18, 2015.
13. Han JY, Fan JY, Horie Y, Miura S, Cui DH, Ishii H, Hibi T, Tsuneki H and Kimura I: Ameliorating effects of compounds derived from Salvia miltiorrhiza root extract on microcirculatory disturbance and target organ injury by ischemia and reperfusion. Pharmacol Ther 117: 280-295, 2008.
14. Xu M, Cao F, Liu L, Zhang B, Wang Y, Dong H, Cui Y, Dong M, Xu D, Liu Y, *et al*: Tanshinone IIA-induced attenuation of lung injury in endotoxemic mice is associated with reduction of hypoxia-inducible factor 1alpha expression. Am J Respir Cell Mol Biol 45: 1028-1035, 2011.
15. Cheng J, Chen T, Li P, Wen J, Pang N, Zhang L and Wang L: Sodium tanshinone IIA sulfonate prevents lipopolysaccharide-induced inflammation via suppressing nuclear factor-kappaB signaling pathway in human umbilical vein endothelial cells. Can J Physiol Pharmacol 96: 26-31, 2018.
16. Pascual M, Ibanez F and Guerri C: Exosomes as mediators of neuron-glia communication in neuroinflammation. Neural Regen Res 15: 796-801, 2020.
17. Rong S, Wang L, Peng Z, Liao Y, Li D, Yang X, Nuessler AK, Liu L, Bao W and Yang W: The mechanisms and treatments for sarcopenia: Could exosomes be a perspective research strategy in the future? J Cachexia Sarcopenia Muscle 11: 348-365, 2020.
18. Li X, Li C, Zhang L, Wu M, Cao K, Jiang F, Chen D, Li N and Li W: The significance of exosomes in the development and treatment of hepatocellular carcinoma. Mol Cancer 19: 1, 2020.
19. Ibrahim A and Marbán E: Exosomes: Fundamental biology and roles in cardiovascular physiology. Ann Rev Physiol 78: 67-83, 2016.
20. Yao X, Wei W, Wang X, Chenglin L, Björklund M and Ouyang H: Stem cell derived exosomes: microRNA therapy for age-related musculoskeletal disorders. Biomaterials 224: 119492, 2019.
21. Cheng N, Du D, Wang X, Liu D, Xu W, Luo Y and Lin Y: Recent advances in biosensors for detecting cancer-derived exosomes. Trends Biotechnol 37: 1236-1254, 2019.
22. Ruan XF, Li YJ, Ju CW, Shen Y, Lei W, Chen C, Li Y, Yu H, Liu YT, Kim IM, *et al*: Exosomes from Suxiao Jiuxin pill-treated cardiac mesenchymal stem cells decrease H3K27 demethylase UTX expression in mouse cardiomyocytes in vitro. Acta Pharmacol Sin 39: 579-586, 2018.
23. Ruan XF, Ju CW, Shen Y, Liu YT, Kim IM, Yu H, Weintraub N, Wang XL and Tang Y: Suxiao Jiuxin pill promotes exosome secretion from mouse cardiac mesenchymal stem cells in vitro. Acta Pharmacol Sin 39: 569-578, 2018.
24. Maremanda KP, Sundar IK and Rahman I: Protective role of mesenchymal stem cells and mesenchymal stem cell-derived exosomes in cigarette smoke-induced mitochondrial dysfunction in mice. Toxicol Appl Pharmacol 385: 114788, 2019.
25. Livak KJ and Schmittgen TD: Analysis of relative gene expressiion data using real-time quantitative PCR and the 2(-Delta Delta C(T)) method. Methods 25: 402-408, 2001.
26. Niu XL, Ichimori K, Yang X, Hirota Y, Hoshiai K, Li M and Nakazawa H: Tanshinone II-A inhibits low density lipoprotein oxidation in vitro. Free Radic Res 33: 305-312, 2000.
27. Tang F, Wu X, Wang T, Wang P, Li R, Zhang H, Gao J, Chen S, Bao L, Huang H and Liu P: Tanshinone II A attenuates atherosclerotic calcification in rat model by inhibition of oxidative stress. Vascul Pharmacol 46: 427-438, 2007.
28. Yin X, Yin Y, Cao FL, Chen YF, Peng Y, Hou WG, Sun SK and Luo ZJ: Tanshinone IIA attenuates the inflammatory response and apoptosis after traumatic injury of the spinal cord in adult rats. PLoS One 7: e38381, 2012.
29. Barnes PJ: Development of new drugs for COPD. Curr Med Chem 20: 1531-1540, 2013.
30. Bartel DP: MicroRNAs: Genomics, biogenesis, mechanism, and function. Cell 116: 281-297, 2004.
31. Ambros V: MicroRNA pathways in flies and worms: Growth, death, fat, stress, and timing. Cell 113: 673-676, 2003.
32. Kloosterman WP and Plasterk RH: The diverse functions of microRNAs in animal development and disease. Dev Cell 11: 441-450, 2006.
33. Hu H, Zhu X and Lin X: GuaLou GuiZhi decoction represses LPS-induced BV2 activation via miR-155 induced inflammatory signals. Pak J Pharm Sci 33: 403-408, 2020.
34. Lin F, Chen HW, Zhao GA, Li Y, He XH, Liang WQ, Shi ZL, Sun SY, Tian PP, Huang MY and Liu C: Advances in research on the circRNA-miRNA-mRNA network in coronary heart disease treated with traditional Chinese medicine. Evid Based Complement Alternat Med 17: 8048691, 2020.
35. Tang C, Zhao R, Ni H, Zhao K, He Y, Fang S and Chen Q: Molecule mechanisms of Ganoderma lucidum treated hepatocellular carcinoma based on the transcriptional profiles and miRNA-target network. Biomed Pharmacother 125: 110028, 2020.
36. Wang X, Chi J, Dong B, Xu L, Zhou Y, Huang Y, Sun S, Wei F, Liu Y, Liu C, *et al*: miR-223-3p and miR-22-3p inhibit monosodium urate-induced gouty inflammation by targeting NLRP3. Int J Rheum Dis 24: 599-607, 2021.
37. Hu Z, Lv X, Chen L, Gu X, Qian H, Fransisca S, Zhang Z, Liu Q and Xie P: Protective effects of microRNA-22-3p against retinal pigment epithelial inflammatory damage by targeting NLRP3 inflammasome. J Cell Physiol 234: 18849-18857, 2019.
38. Chai X, Si H, Song J, Chong Y, Wang J and Zhao G: miR-486-5p inhibits inflammatory response, matrix degradation and apoptosis of nucleus pulposus cells through directly targeting FOXO1 in intervertebral disc degeneration. Cell Physiol Biochem 52: 109-118, 2019.
39. Yamada K, Takizawa S, Ohgaku Y, Asami T, Furuya K, Yamamoto K, Takahashi F, Hamajima C, Inaba C, Endo K, *et al*: MicroRNA 16-5p is upregulated in calorie-restricted mice and modulates inflammatory cytokines of macrophages. Gene 725: 144191, 2020.

40. Ruan C, Cong RJ, Wang M, Wang L, Yu Y, Li X and Lv H: miR-27b-3p targeting BDNF inhibits TrkB/CREB signaling pathway and improves IL-1 β induced chondrocytic inflammation. Preprints: 2021020602, 2021. doi: 10.20944/preprints202102.0602.v1
41. Tian F, Wang J, Ouyang T, Lu N, Lu J, Shen Y, Bai Y, Xie X and Ge Q: miR-486-5p serves as a good biomarker in nonsmall cell lung cancer and suppresses cell growth with the involvement of a target PIK3R1. Front Genet 10: 688, 2019.
42. Yang S, Sui J, Liu T, Wu W, Xu S, Yin L, Pu Y, Zhang X, Zhang Y, Shen B and Liang G: Expression of miR-486-5p and its significance in lung squamous cell carcinoma. J Cell Biochem 120: 13912-13923, 2019.
43. Zhang Y, Fu J, Zhang Z and Qin H: miR-486-5p regulates the migration and invasion of colorectal cancer cells through targeting PIK3R1. Oncol Lett 15: 7243-7248, 2018.
44. Huang XP, Hou J, Shen XY, Huang CY, Zhang XH, Xie YA and Luo XL: MicroRNA-486-5p, which is downregulated in hepatocellular carcinoma, suppresses tumor growth by targeting PIK3R1. FEBS J 282: 579-594, 2015.
45. Mirza-Aghazadeh-Attari M, Ekrami EM, Aghdas SAM, Mihanfar A, Hallaj S, Yousefi B, Safa A and Majidinia M: Targeting PI3K/Akt/mTOR signaling pathway by polyphenols: Implication for cancer therapy. Life Sci 255: 117481, 2020.
46. Sun K, Luo J, Guo J, Yao X, Jing X and Guo F: The PI3K/AKT/mTOR signaling pathway in osteoarthritis: A narrative review. Osteoarthritis Cartilage 28: 400-409, 2020.
47. Pirozzi F, Ren K, Murabito A and Ghigo A: PI3K signaling in chronic obstructive pulmonary disease: Mechanisms, targets, and therapy. Curr Med Chem 26: 2791-2800, 2019.
48. Marwick JA, Chung KF and Adcock IM: Phosphatidylinositol 3-kinase isoforms as targets in respiratory disease. Ther Adv Respir Dis 4: 19-34, 2010.
49. Cerami E, Gao J, Dogrusoz U, Gross BE, Sumer SO, Aksoy BA, Jacobsen A, Byrne CJ, Heuer ML, Larsson E, *et al*: The cBio cancer genomics portal: an open platform for exploring multidimensional cancer genomics data. Cancer Discov 2: 401-404, 2012.